TIME SCALE AND MOLECULAR WEIGHT DISTRIBUTION CONTRIBUTIONS TO DILUTE POLYMER SOLUTION FLUID MECHANICS

Neil S. Berman* and William K. George**

ABSTRACT

Experimental results on drag reduction in pipe flow, pitot tube errors and polymer degradation are presented to support a thickened buffer zone model for dilute polymer solutions. The proposed model exhibits onset when the flow time scale equals the polymer time scale and increased drag reduction, degradation or pitot tube error as increased fractions of the polymers in the distribution are stretched by the flow. Eventually a limit is reached when the measure of increased buffer layer thickness or increased effective viscosity in a pipe flow core, $c[\eta]$, reaches a limit due to entanglement of stretched molecules. The model correlates well with the experimental data.

INTRODUCTION

The addition of small amounts of certain polymers to a solvent results in a large change in the fluid mechanics compared to the solvent alone. In turbulent pipe flow the drag of the dilute polymer solution is reduced as much as a factor of ten below that of the pure solvent. Pressure measurements may differ by a factor of two or more and the stability of flows is also affected. Although the promise of engineering applications of drag reduction has stimulated considerable experimental investigation, the phenomenon is still poorly understood.

A recent review by Lumley [1] summarizes the present understanding of the effect of the high molecular weight additives and also lists references to many of the experimental studies. Among the aspects which must be explained by any theory are onset, the increase in drag reduction or in pressure measurement error after onset, and the maximum asymptote. Some of these are discussed by Lumley for the ideal case of monodisperse (single molecular weight species) polymer solutions. In practice, however, only polydisperse polymer solutions are available and interpretation of experimental results is hindered by a lack of knowledge of the distribution.

It is the purpose of the present study to examine the effect of the molecular weight distribution (or polydispersity) on the onset, the maximum asymptotes and the region in between. We present evidence from water tunnel experiments involving pitot tubes, drag models, pipe flow monitoring of drag reduction, and shear degradation which shows that initially the amount of polymer in the distribution that is stretched by the flow determines the behavior. Eventually maximum drag reductions or maximum pitot tube errors are reached, and we propose a stretching limit to explain these asymptotes.

---

*Arizona State University, Tempe, AZ 85281

**Applied Research Laboratory, The Pennsylvania State University, University Park, PA

Reprinted from PROCEEDINGS OF THE [illegible] HEAT TRANSFER AND FLUID MECHANICS INSTITUTE, Lorin R. Davis and Robert E. Wilson, Editors. Stanford University Press, 1974.

THE DISTRIBUTION PROBLEM

Ideally the true molecular weight distribution of a commercial grade polymer should be known and experiments should be carried out for this distribution and for distributions approaching the monodisperse case. Unfortunately the best drag reducers in water are not produced in narrow molecular weight grades and the highest molecular weights are much more effective. Therefore, extremely small amounts of the highest molecular weights distort the drag reduction experiments. An average molecular weight can be assigned to the polymers in solution by measuring the average size by light scattering or intrinsic viscosity. In this study various grades of Polyox, a high molecular weight polyethylene oxide, in water were used. Merrill et al. [2] found the relationship between $[\eta]$, the intrinsic viscosity in deciliters per gram and the average molecular weight for Polyox in water to be

$$[\eta] = 1.03 \times 10^{-4} M^{0.78} \quad , \tag{1}$$

based on light scattering, intrinsic viscosity and the Zimm-Rouse molecular model. The exponent on the molecular weight in the Zimm-Rouse model assuming no solvent interaction would be 0.5. The higher value for the Polyox-water system indicates that there is a strong interaction and the Polyox molecules are swollen to perhaps their maximum extent.

The average molecular weight obtained from the intrinsic viscosity is normally used to characterize the particular polymer. Polyox WSR 301 has an intrinsic viscosity of from 10-30 deciliters per gram depending upon the blend and age. The average molecular weight from Eq. (1) is 2.5×10^6 to 10^7. Another polymer used in these studies was Polyox WSR N80. The intrinsic viscosity was found to be 1.8 deciliters per gram which corresponds to an average molecular weight of 2.7×10^5. For Polyox in water these average molecular weights from intrinsic viscosity approach the weight average molecular weights from the second moment of the distribution. However, any comparison of Polyox WSR 301 and WSR N80 must consider the entire distribution.

It is possible to obtain the distribution from light scattering or gel chromatography measurements. Difficulties have been encountered with the Polyox-water system in gel chromatography and the light scattering method is not developed to the point where it can be used as a standard. In fact gel chromatography and light scattering for polymers are often calibrated from intrinsic viscosity measurements on narrow polystyrene fractions. We therefore propose using pipe flow drag reduction itself as a qualitative (for the present) standard of comparison.

Figure 1 shows some typical curves of friction coefficient vs. Reynolds number for Polyox WSR 301 ($[\eta] \sim 12$ deciliters per gram) and Polyox WSR N80 ($[\eta] \sim 1.8$ deciliters per gram) in a 6.35mm (1/4 inch) smooth pipe. Note that the N80 curve displays a well defined breakoff from the standard curve for water and that a considerably higher concentration compared to the 301 is necessary to obtain significant drag reduction. In order to obtain an "onset" for Polyox 301 it is necessary to extrapolate the curve back to the pure water line. At sufficiently high concentrations an apparent maximum drag reduction is reached and the solution is always at maximum drag reduction. At intermediate concentrations the curve may reach the maximum drag reduction line and remain on it or follow the curves above the maximum drag reduction line. Reasons for some of this behavior will be discussed later. We can safely assume that the onset behavior is established by the highest molecular weight fraction in the polymer distribution. The application of any single average molecular weight, time

scale or radius of gyration as a correlating parameter is bound to end in failure. Berman and George [3] have shown that "onset" is clearly related to the molecular time scale. The terminal relaxation time of the molecule from the Zimm-Rouse theory is

$$T_1 \alpha \frac{\mu_s[\eta]M}{RT} \tag{2}$$

For a distribution we would have many such time scales. If we use the same distribution but change μ_s, by adding glycerine to the water solution we obtain the results in Table I, showing the relationship between onset and the molecular time scale, and no relationship between onset and radius of gyration. The data of Berman and George also show that the entire curve such as the one for 425 ppm of Polyox N80 in Fig. 1 is displaced. All the time scales in the distribution are affected. We can now conclude that the behavior of the drag reduction curve immediately after onset can be related to the molecular weight distribution.

It is also important to recognize that Polyox WSR 301 has a wide molecular weight distribution but does not have as much of a high molecular weight tail as other drag reducing polymers with "narrower" distributions, such as Polyox N80. There is an upper limit to the molecular size of the polyethylene oxide and the high average molecular weight WSR 301 has a significant fraction near this upper limit. The low average molecular weight N80 has a long tail on the distribution extending out to the limit. We can then see that onset should not be a point at all but a continuous curve and that it takes a larger amount of lower average molecular weight material to obtain drag reduction because enough of the high molecular weight tail must be present so that drag reduction can be observed. It is not surprising that previous correlations [4] could not resolve the time scale--length scale controversy.

EXPERIMENTAL STUDIES

To see how the pipe flow drag reduction--time scale distribution characterization works in other flow situations we performed some experiments on pitot tube errors and drag on a three inch cylindrical model in the 12 inch water tunnel at the Garfield Thomas Water Tunnel, State College, Pennsylvania.

The experiments were run using from 1-100 parts per million by weight (ppm) solutions of Polyox WSR 301. First about 400 gallons of a concentrated solution were prepared and this was added to the fill water to the tunnel to give the final concentration. The 6.35mm (1/4 inch) tube was connected to the tunnel so a semi-continuous check on the drag reduction in pipe flow could be monitored. This was necessary as the polymer solution degraded as the tunnel was run. Therefore, we could run experiments on many different polymer solutions as time progressed.

At the same time that the pressures across the tunnel nozzle and at the pitot tube taps were measured, a flow rate vs. pressure drop curve was obtained for the solution in the tunnel. A schematic diagram of the experimental apparatus is shown in Fig. 2. The operating procedure was as follows:

1. A pressure difference is created between the tunnel and the empty receiver by running the tunnel at 5-20 psi above atmospheric pressure.

2. Flow is initiated by opening the valve. The pipe pressure drop and receiver weight were recorded alternately at one second intervals for

approximately 50 seconds. The signals were integrated over the one second to smooth rapid fluctuations.

3. The averaged wall shear stress and mass flow rate were calculated for the same instant in time and plotted. This part was done on an IBM 1130 computer.

The receiver size was large enough so that for the flow rates measured, turbulent fluctuations corresponding to the rate of weight change in the receiver did not change significantly at the pressure taps. A typical tunnel run is shown in Fig. 3. Here the plot of wall shear, τ_w/μ vs. flow rate, Q, is used as the time scale is related to the wall shear. We ignore the slight change in viscosity of the solution with polymer addition.

Pitot Tube Error

The pitot tube experiment has been detailed by Berman, Gurney and George [5]. We have replotted the data in Fig. 4 to show clearly the correlation between the extrapolated onset time scale and the onset of pitot tube error. A 1/16 inch standard Prandtl type pitot static tube was used and the tunnel velocity was changed to vary the flow time scale. The top curve of pitot tube error corresponds to fresh polymer when maximum drag reduction was observed in pipe flow. These maximum errors increase almost linearly with velocity. Then the relative error in velocity would decrease since velocity is proportional to the square root of the total pressure difference between the taps of the pitot tube. At velocities of one meter/sec. the error would be 100%, although at the velocities shown on Fig. 4 the error is less than 10%.

Stretching of polymer molecules in an irrotational flow field such as the pitot tube nose has been predicted by Lumley [6]. The polymers should become stretched when the strain rate, 2U/D, becomes greater than the reciprocal of the molecular time scale. Figure 4 shows that this is indeed the case. We also show that the behavior after onset is similar for pipe flow drag reduction and pitot tube errors and that maximum asymptotes are reached in each case.

Polymer Degradation

The next experiment concerned the degradation of the polymer solution and the drag on the cylindrical body. A pump jet was placed in the tunnel and a constant percentage of the polymer was passed through it on each circuit. Drag was monitored on a 3 inch diameter cylinder with a rounded nose and tapered afterbody, placed before the pump jet in the flow circuit. The drag on the model was monitored as well as the drag reduction in the small pipe. In previous studies without the pump jet as a degrader, degradation proceeded as in Fig. 3. The shear rate on the model was too large to use the pipe flow onset characterization, but deviation from the maximum drag reduction curve did correlate with the fall off from maximum drag on the model at the average shear rate of the model. This value was of the order 5×10^4 sec.$^{-1}$ at fall off. As the polymer in the tunnel degraded the average shear on the model increased and the monitoring of drag on the 3 inch model proved to be a better characterization than the pipe flow. At the higher shear rate in the turbulent boundary layer of the model lower molecular weight polymers could be stretched than in the pipe flow. The data can then be presented in the form of drag reduction on the model vs. time for constant degrader performance. The measured drag on the model must be corrected for the form drag to make such a plot meaningful. This has been done on Fig. 5 assuming a constant form drag which is not affected by the polymer solution. Such an assumption is questionable, but the only one possible without extensive further studies.

THEORY

If one parameter can be used to characterize the amount of stretching and if this amount is related to drag reduction, pitot tube error and degradation (assuming that the stretching results in degradation) we have at least indirect support for the theory.

Lumley [1] postulates that drag reduction, D_R, is proportional to buffer layer thickening or $c[\eta]$ for monodispersed polymers. For the polydisperse case we can extend this to

$$D_R \alpha \sum c_i [\eta]_i \tag{3}$$

where the sum is only over those molecules whose terminal relaxation time is greater than the flow time scale.

Lumley's use of $[\eta]$ is related to the intrinsic viscosity of the expanded molecules, however, we assume here that at onset it is proportional to $[\eta]$ for the unexpanded molecule. Also as we show later there may be a limit to the expansion and the true $c[\eta]$ may be difficult to evaluate. For Polyox WSR 301 let us postulate a rectangular distribution

$$\begin{aligned} P(M) &= 1/(M_2-M_1), && M_1 \leq M \leq M_2 \ , \\ &0, && \text{elsewhere.} \end{aligned} \tag{4}$$

then

$$D_R \ \alpha \int_{M_0}^{M_2} c[\eta] \ P(M) dM \tag{5}$$

where we replace the sum by an integral and M_0 $(M_1 \leq M_0 \leq M_2)$ has a time scale corresponding to the flow timescale. For

$$c[\eta] = c_T K M^b \tag{6}$$

where K is a constant and, c_T is the total concentration in parts per million, we obtain

$$D_R \ \alpha \ \frac{c_T (M_2^{b+1} - M_0^{b+1})}{(M_2-M_1)(b+1)} \ . \tag{7}$$

When the distribution is wide, $M_2 >> M_1$, we neglect M_1 in the denominator and using

$$T_1 \ \alpha \ M^{b+1} \ , \tag{8}$$

we have

$$D_R \propto M_2^{\,b}\, c_T \left[1 - \frac{T_o}{(T_1)_2} \right]; \qquad T_o \leq (T_1)_2 \,. \tag{9}$$

This equation predicts onset when $T_o = (T_1)_2$, a linear dependence on concentration, and a dependence on molecular weight of the largest molecules to the same power as the intrinsic viscosity depends on molecular weight. All these predictions have been observed by Paterson and Abernathy [7]. Since real molecular weight distributions are not rectangular, the result must be slightly modified to account for a realistic distribution. For Polyox WSR 301 the distribution is reasonable and the weight average molecular weight is representative of the largest molecules. This model applies after onset but not at maximum drag reduction. Similar calculations for other models (Gaussian and log normal) have been made and show the same dependence on an average molecular weight and total concentration. Onset becomes a gradual phenomenon, but there is an almost linear part of the drag vs. Reynolds number curve which can be extrapolated to give the onset behavior.

If the pitot tube error is also proportional to $c[\eta]$, the rectangular distribution with T_o equal to D/2U predicts

$$\Delta P_e \propto \left[1 - \frac{D}{2U(T_1)_2} \right] ; \qquad \frac{D}{2U} < (T_1)_2 . \tag{10}$$

The variation with U/D corresponds closely to the experimental results on Fig. 3 of Berman, Gurney and George and even predicts the approach to onset. The numerical agreement means only that the time scale for onset of drag reduction and onset of pitot tube error can be made the same. Figure 6 shows the experimental points and Eq. 10 with an appropriate value for the proportionality constant. The polymer time scales were obtained from pipe flow drag reduction data.

The next test of the $c[\eta]$ model with the polymer molecular weight distribution effects is the degradation experiment. To find a suitable degradation rate equation the curves on Fig. 5 can be differentiated. When this is done, plots of $-dD_R/dt$ vs. D_R on log-log graph paper give straight lines all with slopes of 2.3. Then

$$\frac{-dD_R}{dt} = k\, D_R^{\,2.3} \tag{11}$$

where k is a rate constant.

Integrating

$$D_R^{\,-1.3} = 1.3\, kt + K_o \tag{12}$$

From the curves we can obtain the constants given in Table II. We note that $k_2/k_1 = 2.1$ and $k_3/k_2 = 0.58$. Within experimental error then k is proportional to RPM squared and inversely proportional to concentration.

$$k = k_o \, S^2/c_T \tag{13}$$

where S is the shear rate of the degrader assumed to be linearly related to the RPM. Also K_o is essentially constant. This result can be compared to that of Asbeck and Baxter [8]

$$\frac{1}{M} - \frac{1}{M_I} = k/\mu \, S^2 t \tag{14}$$

where M is the average molecular weight and M_1 is the initial average molecular weight. Letting D_R be proportional to $c[\eta]$ and again using $[\eta]$ proportional to $M^{0.78}$ for Polyox, Eq. 12 becomes

$$\frac{1}{M} - K_o' = k_o' \, S^2 t \, c_T^{0.3} \tag{15}$$

The dependence on $c_T^{0.3}$ is minimal and could well have been eliminated making Eq. 15 and Eq. 14 identical. The use of D_R proportional to $c[\eta]$ is again verified. Based on all the forms of indirect evidence, we conclude that the behavior of dilute polymer solutions after the onset of drag reduction as well as after the onset of pitot tube error is indeed proportional to $c[\eta]$.

The degradation experiment also contains information about the mechanism. First the polymers must be stretched before they degrade. When the vorticity is greater than the strain rate as in laminar pipe flow, the molecules are not stretched even if the product of polymer terminal relaxation time and strain rate is greater than one. Turbulent or irrotational flows give conditions where the strain rate of the flow is greater than the vorticity and stretching will take place. The dependence on strain rate squared in Eq. 15 implies a correlation with energy input as suggested in other studies [9]. However, the rate constant k_o' contains the effect of recirculating only approximately 15% of the polymer through the degrader on each pass. Also the strain rate in this degrader was high enough so that most of the molecules in the original distribution were affected.

It is not clear whether degradation proceeds by breaking up the large molecules into tiny pieces or into a combination of small and medium sized pieces. The largest molecules must break up first or the decay in drag reduction would be slower. Other preliminary studies, when all the polymer at a somewhat lower concentration was passed through the degrader, indicate that the molecules are all broken up into tiny pieces and that the appearance of S^2t in the rate equation is only related to the pumping rate. That is if the molecule is stretched enough it breaks into a lot of small pieces. The correlation with energy input is only a measure of how much of the polymer solution passes through the high strain rate field where it is degraded compared with the amount that does not.

THE MAXIMUM ASYMPTOTE

The dependence of drag reduction on $c[\eta]$ continues until $c[\eta]$ becomes large. This is apparent experimentally since a maximum asymptote is reached as shown on Fig. 1. Since only a limited amount of data are available for the pitot tube error we will confine the discussion to pipe flow drag reduction.

Thus far we have been able to correlate experimental observations with the amount of polymer stretched by the flow. The dominating factor has been the distribution of molecular weights or time scales. For monodisperse polymers with only a single time scale Lumley shows that since $c[\eta]$ is increased when the polymer is stretched, small turbulent eddies are suppressed for a larger distance from the wall than the standard sublayer. Then the buffer layer increases in size until the limit of the center of the pipe is reached. When enough polymer is present the drag curve from onset to maximum drag reduction, would be essentially a step function. Experiments do not confirm this mechanism but instead show a gradual increase in drag reduction after onset as shown in Fig. 1. This does not invalidate Lumley's theory but until a monodisperse polymer is available to test it cannot be confirmed.

In some cases the maximum may be related to degradation. That is when the Zimm-Rouse time is reached the molecule is stretched and continues to be stretched by the flow until it breaks or becomes limited by other molecules. This situation is illustrated by the high Reynolds number results of Fig. 1 and shows a marked concentration dependence. Some pipe flow results are adequately explained by degradation. Then the maximum asymptote must be the loci of points like point (a) on Fig. 1, assuming that for Reynolds numbers greater than that at point (a) degradation influences the results.

We are then led to the problem of what is the maximum drag reduction asymptote. Figure 7 shows schematically most results on this subject. If degradation is neglected, and we also neglect experiments with high concentrations of polymers which give an unstable but questionable turbulent flow, the curve C is the maximum asymptote. This is the asymptote generally shown in other references [10]. Lumley postulates that if the molecules expand, the intrinsic viscosity increases until the effective viscosity, $\mu_s(1+c[\eta])$, in the center of the pipe is very large. An experimental observation of Lumley's model would correspond to the high concentration data of Rollin and Seyer [11]. The ultimate drag reduction that has been observed at these very high concentrations, or by redrawing the maximum asymptote only through the lowest points as shown on Fig. 1 gives the lower curve on Fig. 7. This is shown only schematically.

There is another explanation for the observed deviation from the maximum asymptote. This is a limit to $c[\eta]$. Such a limit is reasonable in terms of molecular properties of polymer solutions. For $c[\eta]<<3$ the terminal relaxation time, T_1, is based on interactions between individual parts of the molecule. When $c[\eta]$ approaches 3, the free draining theory takes over and there is no interaction between motions of the submolecule. As $c[\eta]$ increases beyond 3 the molecules no longer act independently and actually overlap when stretched. For $c[\eta]>30$ the molecular motions are affected by entanglement. Detailed descriptions of these phenomena are given by Ferry [12]. To examine the $c[\eta]$ limit along with the extension of the buffer layer to the center of the pipe, the velocity profile data of Rollin and Seyer are plotted on Fig. 8. These authors did not plot the 1000 ppm run on the u_+ vs. y_+ coordinates so we have done so. This curve confirms Lumley's theory that the buffer layer extends to the center of the pipe. For drag reduction less than the maximum, illustrated by the 100 ppm line, a log profile in the center parallel to that for the pure solvent exists. Huang and Santelli [10] calculated the friction factor--Reynolds number relationship for maximum drag reduction assuming a "strongly interacting layer" dominates. The result is similar to using the 1000 ppm run of Rollin and Seyer or assuming the sublayer extends to the pipe center. We obtain

$$u_+ = 34 \log y_+ - 25.5 \tag{16}$$

for the maximum drag line.

Experimentally almost all data on drag reduction ([7], [10]) show deviations from the maximum asymptote at high Reynolds numbers. For Polyox WSR 301 these deviations all occur at Reynolds numbers about 20,000, independent of pipe size and concentration. This does not correlate with the idea of degradation but is consistent with the stretching limit.

We can assume that the maximum drag reduction asymptote is indeed as explained by Lumley. However, before the viscosity in the pipe center increases to give the maximum drag reduction line, the limiting value of $c[\eta]$ can be reached. From concentrated polymer solution results discussed by Ferry this limit should be about 30. This limit occurs when the Reynolds stress becomes greater than the viscous stress at the centerline and the sublayer no longer can extend to the pipe center. Since the Reynolds stress increases faster with Reynolds number than the viscous stress, at a high enough Reynolds number the polymer solution drag curve should always deviate from the maximum drag reduction. The effective viscosity, ν_{eff}, in the pipe center is

$$\frac{\nu_{eff}}{\nu} = 1 + c[\eta] \tag{17}$$

where $[\eta]$ is the intrinsic viscosity of the stretched molecules. The condition for staying on the maximum asymptote is

$$\overline{uv} < \nu_{eff} \frac{\partial U}{\partial y} \tag{18}$$

Using the scale relationships for turbulent pipe flow given by Tennekes and Lumley [13], we can replace $-\overline{uv}$ by u_*^2. From Eq. 16 $-\frac{dU}{dy}$ is 15 u_*/y. Then Eq. 18 becomes

$$u_*^2 < 15\, \nu_{eff}\, u_*/y \quad . \tag{19}$$

Multiplying both sides by the integral scale, ℓ, gives at the center

$$R_\ell = \frac{u_* \ell}{\nu_{eff}} < 30 \frac{\ell}{D} \tag{20}$$

or for $\ell = D/2$, we have

$$R_\ell < 15 \tag{21}$$

This corresponds to the point where the Taylor microscale equals the integral scale which is consistent with the picture of the suppression of small eddies.

For $R_\ell > 15$ the maximum asymptote cannot be maintained. If we take $u_*/U_m \sim .05$, we have

$$N_{Re} = \frac{DU_m}{\nu} < 600 \frac{\nu_{eff}}{\nu} \quad , \tag{22}$$

at the experimental point of deviation of $N_{Re} \sim 20{,}000$

$$\frac{\nu eff}{\nu} \sim 37 \tag{24}$$

or

$$c[\eta] \sim 36 \tag{25}$$

The experimental evidence, therefore, points to a deviation from maximum drag reduction at precisely the point where entanglements are expected to occur.

CONCLUSIONS

We have presented a combination of experiments and theory to give a reasonable explanation of the observed fluid mechanical behavior of dilute polymer solutions. When the polymer time scale becomes equal to the flow time scale, onset of drag reduction or pitot tube error occurs. For polydisperse polymers the behavior when this onset time is passed (flow time scale is reduced) is governed by the amount of polymer in the distribution which can be stretched. An excellent correlation can be obtained if the sublayer thickening, or $c[\eta]$ for the stretched molecules which is proportional to it, is used along with a distribution function. If molecules can be continued to be stretched by the flow indefinitely, the buffer layer would be extended indefinitely also. The result would be maximum asymptotes eventually resembling an intermittent laminar flow. At low Reynolds numbers enough polymers can be stretched to reach this asymptote before another limit, the entanglement limit, is reached. The entanglement limit of $c[\eta] \sim 30$ is an upper bound and limits further stretching of the polymers. As the Reynolds number increases the drag curve departs from the maximum asymptote and the behavior is governed by the $c[\eta]$ limit. If the Reynolds number is too high before the polymers are stretched, the maximum asymptote will never be reached. A combination of polymer molecule breakage, number stretched and the $c[\eta]$ limit governs the behavior of high Reynolds numbers.

ACKNOWLEDGEMENTS

This work was partially supported by the Applied Research Laboratory of the Pennsylvania State University under contract with the Naval Ordnance Systems Command and the General Hydromechanics Research Program of the Naval Ship Systems Command.

NOMENCLATURE

c_i = concentration of polymer of molecular weight M_i

c = concentration

c_T = total concentration

D = diameter

D_R = drag reduction

f = friction coefficient, $2u_*^2/U_m^2$

ℓ = integral scale

M = molecular weight or average molecular weight

M_I = initial molecular weight

N_{Re} = Reynolds number $U_m D/\nu$

$P(M)$ = distribution function

R_e = Reynolds number $u_* \ell/\nu$

R = gas constant

S = shear rate

T = absolute temperature

T_1 = terminal relaxation time

$\overline{T}_1$ = average time scale

T_o = onset time scale

t = time

U = local mean velocity

U_m = average velocity from flow rate

u_* = friction velocity, $\sqrt{\tau_w/\rho}$

u_+ = dimensionless velocity, U/u_*

u = axial velocity fluctuation

v = radial velocity fluctuation

y_+ = dimensionless distance from wall $y\ u_*/\nu$

y = distance from wall

ΔP_e = pitot tube error

$[\eta]$ = intrinsic viscosity

μ = dynamic viscosity of solution

μ_s = dynamic viscosity of solvent

ν = kinematic viscosity

ν_{eff} = effective kinematic viscosity of the solution of stretched polymer

τ_w = wall shear

Percent Glycerine	μ_s, Viscosity g/cm sec	$[\eta]$ Deciliters/g	Onset u_*2/ν sec^{-1}	Onset $\mu_s[\eta]u_*^2/\nu$ cm^2/sec^2
0	.009	1.8	8000	13,000
25	.014	1.65	6000	14,000
53	.059	1.3	1700	13,000

TABLE I. Onset data for 425 ppm solutions of Polyox WSR N-80. The last column should be constant if onset is related to the time scales, and the u_*^2/ν column should be constant if onset is related to the length scales. The addition of glycerine changes the viscosity much more than the intrinsic viscosity. The polymer time scale is proportional to $\mu_s[\eta]$ and the length scale to the cube root of $[\eta]$.

Test	RPM	Velocity ft/sec	Conc. ppm	k	K_o
1	2250	25	50	8.969×10^{-5}	2.57×10^{-3}
2	2250	25	20	1.888×10^{-4}	2.87×10^{-3}
3	1750	20	20	1.0913×10^{-4}	2.92×10^{-3}

TABLE II. Degradation tests in the 12 inch water tunnel using a pump jet degrader. About 15% of the total flow went through the degrader on each pass.

REFERENCES

1. Lumley, J. L. Drag Reduction in Turbulent Flow by Polymer Additives, Macromolecular Reviews, in press.

2. Merrill, E. W., K. A. Smith, H. Shin and H. S. Mickley. Study of Turbulent Flows of Dilute Polymer Solutions in a Couette Viscometer, Trans. Soc. Rheology, 1966, 10, 335.

3. Berman, N. S. and W. K. George. Onset of Drag Reduction in Dilute Polymer Solutions, Phys. Fluids, in press.

4. Virk, P. S. and E. W. Merrill. The Onset of Dilute Polymer Solution Phenomena in Viscous Drag Reduction in C. S. Wells, Ed. Viscous Drag Reduction New York: Plenum Press, 1969.

5. Berman, N. S., G. B. Gurney and W. K. George. Pitot Tube Errors in Dilute Polymer Solutions, Phys. Fluids, 1973, 16 (9), 1526-1528.

6. Lumley, J. L. Centerline Bernoulli Equation for Quasisteady Dilute Polymer Flow, Phys. Fluids, 1972, 15 (2), 217-219.

7. Paterson, R. W. and F. H. Abernathy. Turbulent Flow Drag Reduction and Degradation with Dilute Polymer Solutions, J. Fluid Mech., 1970, 43, 689-710.

8. Asbeck, W. K. and M. K. Baxter in F. E. Bailey and J. V. Koleske. Configuration and Hydrodynamic Properties of the Polyoxyethylene Chain in Solution. Chap. 23 in Martin J. Schiek, ed., Nonionic Surfactants, New York: Marcel Dekker Inc., 1967, p 805.

9. Wilhelmi, George F. "An Experimental Investigation of Centrifugal Pump Performance and Polymer Degradation Effects with Dilute Polyox WSR-301 Solutions," Research and Development Report 3912. Bethesda, Md: Naval Ship Research and Development Center, 1973.

10. Huang, T. T. "Similarity Laws for Turbulent Flow of Dilute Solutions of Drag Reducing Polymers," Research and Development Report 4096. Bethesda, Md: Naval Ship Research and Development Center, 1973.

11. Rollin, A. and F. A. Sayer. Velocity Measurements in Turbulent Flow of Viscoelastic Solutions, Canadian J. of Chem. Eng., 1972, 50, 714-718.

12. Ferry, John D. Viscoelastic Properties of Polymers. New York: John Wiley, 1961.

13. Tennekes, H. and J. L. Lumley. A First Course in Turbulence. Cambridge, Mass.: the MIT Press, 1972.

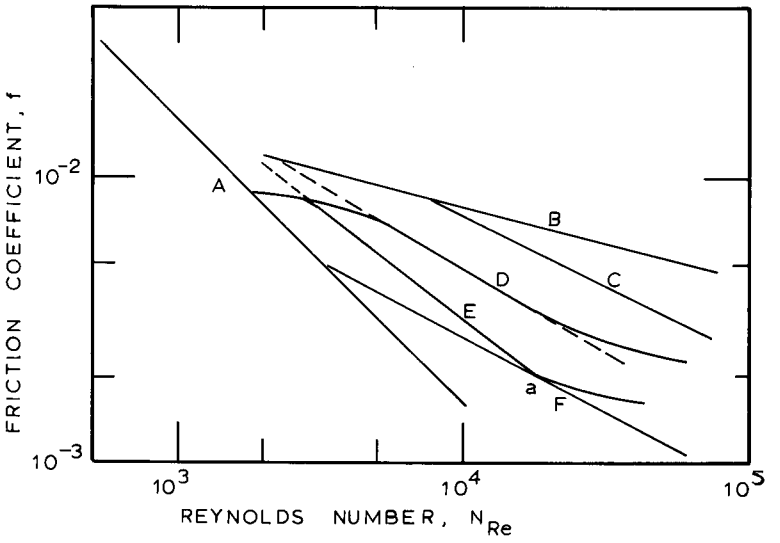

FIGURE 1 Pipe Flow Friction Coefficient vs. Reynolds Number Showing Typical Drag Reduction of Dilute Polymer Solutions. Curve A, Laminar Flow; B, Turbulent Solvent Alone; C, 425 ppm Polyox WSR N80 in Water; D, 8 ppm Polyox WSR 301 in Water; E, 16 ppm Polyox WSR 301 in Water; and F, the Maximum Drag Reduction Asymptote. The Dotted Lines are Extrapolations of the Straight Line Part of the curves. Point (a), as Explained in the Text, Shows a Deviation From the Maximum Asymptote.

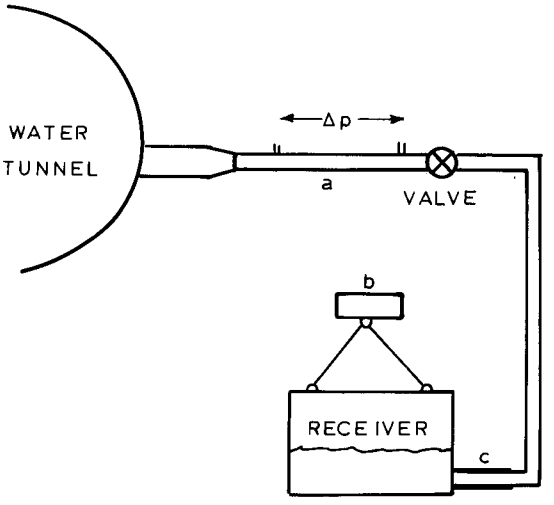

FIGURE 2 Schematic of Continuous Pipe Flow Drag Reduction Monitor. (The Letters Refer to a, the 1/4 Inch Inside Diameter Tube Six Feet Long With Entrance Trip Ring and Pressure Taps 55 Inches Apart; b, the Strain Gauge Weight Measuring Cell; and c, Flexible Coupling.)

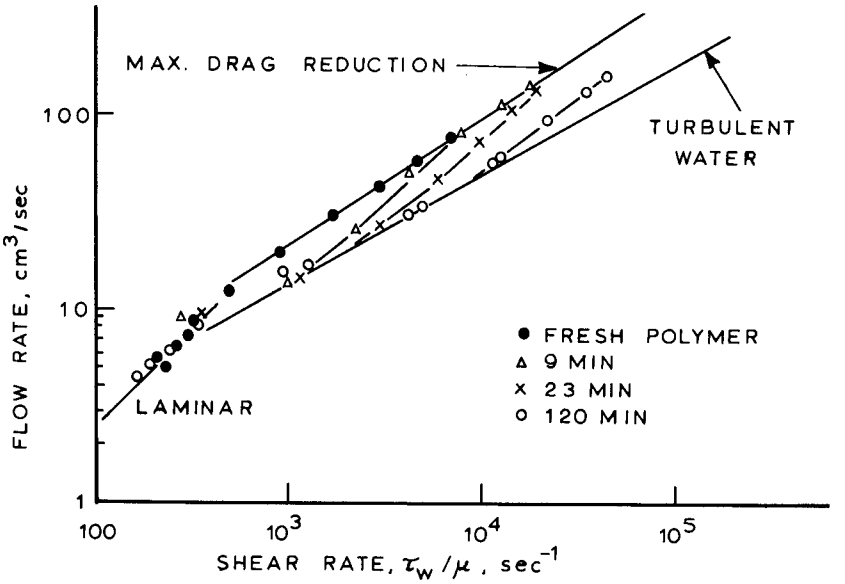

FIGURE 3 Record of Polymer Drag Reduction for the 12-Inch Water Tunnel Running at 30 Feet per Second with Polymer Concentration 100 ppm Polyox WSR 301 in Water. Times for the Data Points are After the Start of the Run.

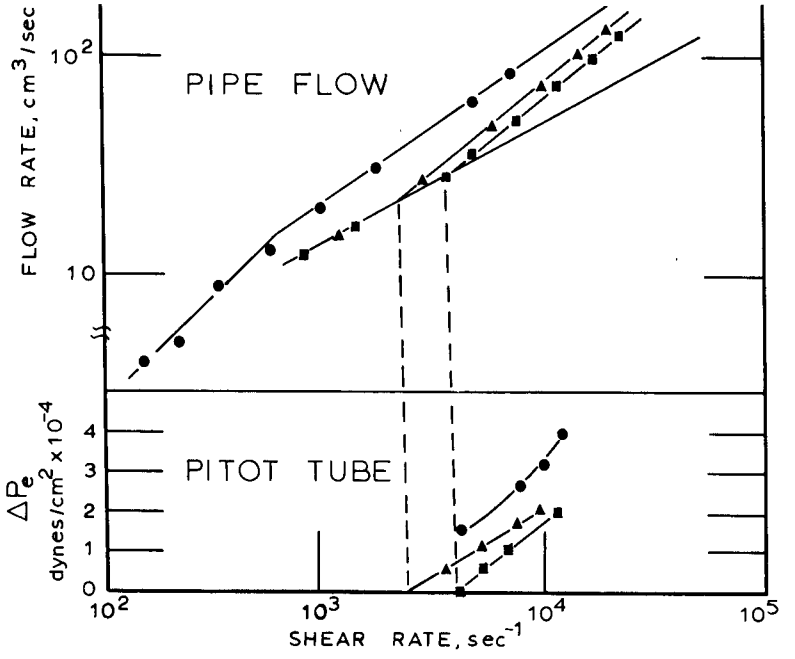

FIGURE 4 Onset Shear Rates (u_*^2/ν for Pipe Flow and 2U/D for Pitot Tube Errors) and Maximum Asymptotes for Pipe Flow Drag Reduction and Pitot Tube Errors. The Same Symbols on the Curves are for the Same Polymer Solution. Solid Circles are on the Maximum Asymptote. Dotted Lines Compare onset points.

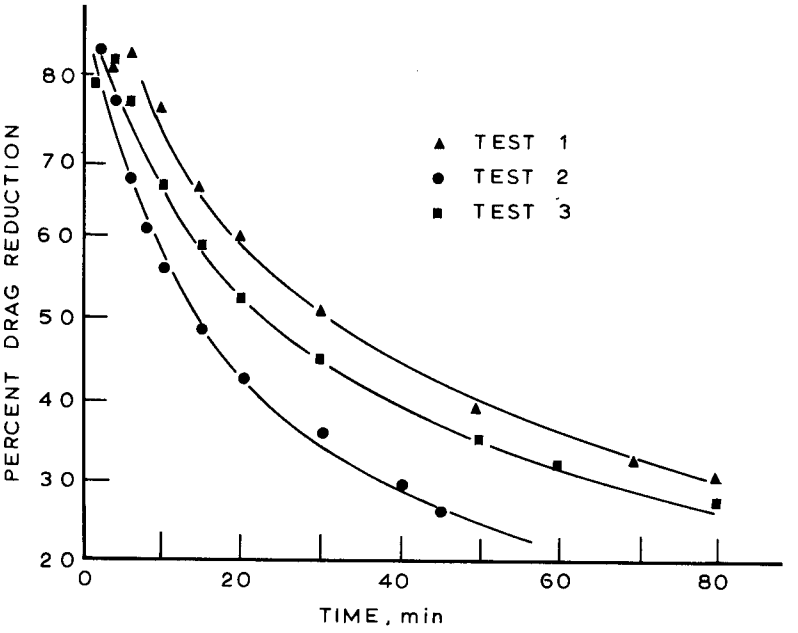

FIGURE 5 Polymer Degradation Monitored by Drag Reduction on a 3-inch Body in the 12-inch Water Tunnel with a Pump Jet Degrader. Test Conditions are given in Table II. The Lines are Based on Eq. 12 and the Constants of Table II.

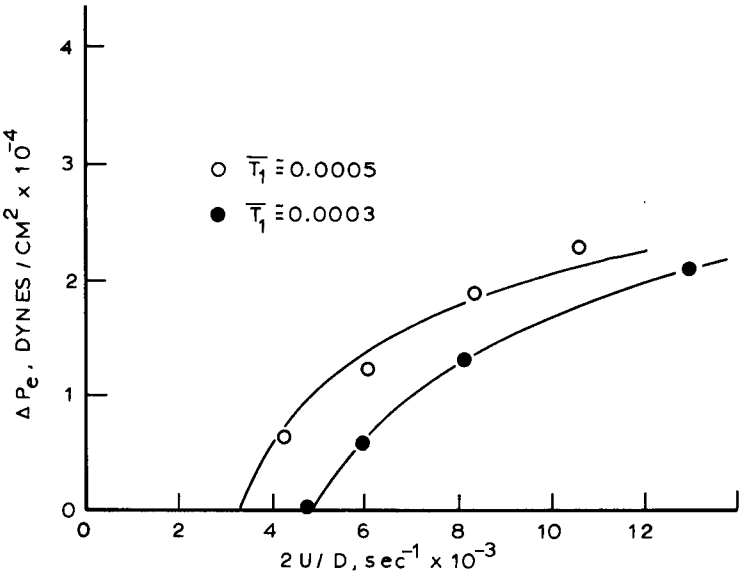

FIGURE 6 Comparison of Pitot Tube Error Data with Theory. The Average Time Scales are Related to Pipe Flow Drag Reduction. The Lines are Eq. 10 with $(T_1)_2$ Taken as the Zero Error Intercept.

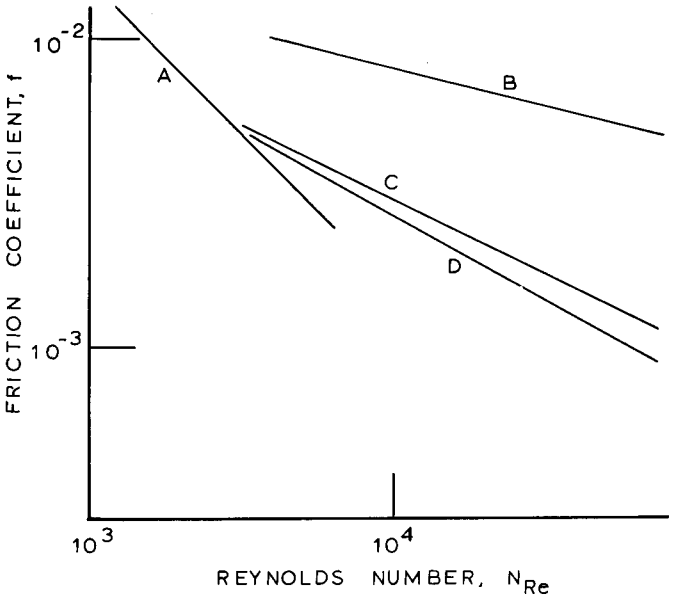

FIGURE 7 Comparison of Maximum Drag Reduction Models. A is Laminar Flow; B, Standard Turbulent Curve; C, Maximum Asymptote from Many Experimental Observations not Including High Concentrations of Polymer; D, Maximum Asymptote Assuming the Sublayer Extends to the Pipe Center.

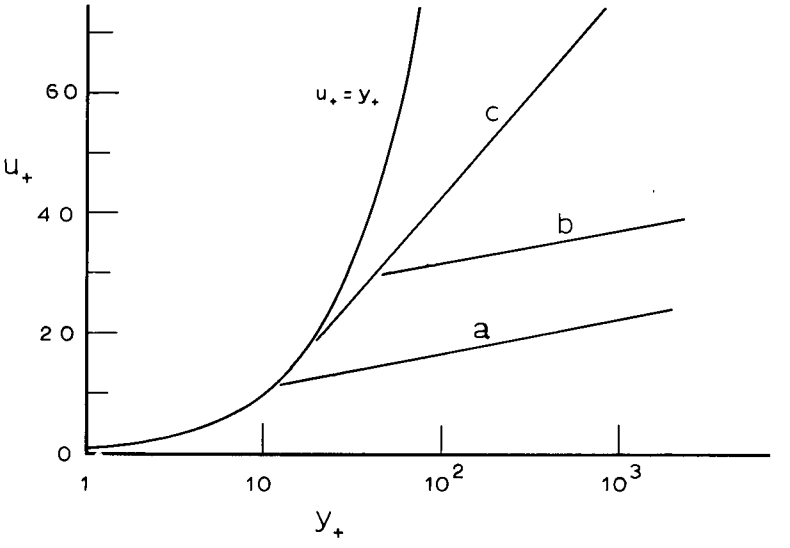

FIGURE 8 Turbulent Velocity Profiles for Pipe Flow Showing a, Solvent Profile $u_+ = 5.75 \log y_+ + 5.5$; b, Typical Drag Reduction Profile not Maximum Drag Reduction (100 ppm Separan AP30 at 60% Drag Reduction, $N_{Re} = \overline{80,000}$ [11]); c, Maximum Drag Reduction When Sublayer Extends Near Pipe Center. (1000 ppm Separan AP30 at 83% Drag Reduction, $N_{Re} = 65,000$ [11]).